Chemical ordering beyond the superstructure in long-range ordered systems

2016 New J. Phys. 18 113051

(http://iopscience.iop.org/1367-2630/18/11/113051)

IOP Publishing New J. Phys. 18 (2016) 113051 doi:10.1088/1367-2630/18/11/113051

New Journal of Physics
The open access journal at the forefront of physics

Deutsche Physikalische Gesellschaft DPG
IOP Institute of Physics

Published in partnership with: Deutsche Physikalische Gesellschaft and the Institute of Physics

OPEN ACCESS

RECEIVED
17 September 2016

REVISED
25 October 2016

ACCEPTED FOR PUBLICATION
11 November 2016

PUBLISHED
29 November 2016

PAPER

Chemical ordering beyond the superstructure in long-range ordered systems

Markus Stana[1,4], **Bogdan Sepiol**[1], **Rafał Kozubski**[2] **and Michael Leitner**[3,4]

[1] Universität Wien, Fakultät für Physik, Boltzmanngasse 5, 1090 Wien, Austria
[2] M. Smoluchowski Institute of Physics, Jagiellonian University in Krakow, Reymonta 4 30-059 Krakow, Poland
[3] TU München, Physik-Department E13, 85747 Garching, Germany
[4] Authors to whom any correspondence should be addressed.

E-mail: markus.stana@univie.ac.at **and** michael.leitner@frm2.tum.de

Keywords: short-range order, long-range order, Warren–Cowley parameters, intermetallics, alloy

Abstract

To describe chemical ordering in solid solutions systems Warren–Cowley short-range parameters are ordinarily used. However, they are not directly suited for application to long-range ordered systems, as they do not converge to zero for large separations. In this paper, the theory is generalized to long-range ordered systems and chemical short-range order beyond the superstructure arrangements is discussed quantitatively on the example of a non-stoichiometric B2-ordered intermetallic alloy. Parameters of interatomic potentials are taken from an embedded atom method calculations and the degree of order is simulated by the Monte Carlo method. Both on-lattice and off-lattice methods, where the latter allows individual atoms to deviate from their regular lattice sites, were used, and the resulting effects are discussed.

1. Introduction

In elemental systems consisting of one type of atom, the structural configuration on the atomic scale in principle is defined by the crystal lattice. In contrast, in multi-component systems aspects of order give rise to additional degrees of freedom. On the one hand, this pertains to long-range order, where the crystal structure's sublattices have different elemental make-ups. On the other hand, short-range order corresponds to energetically preferred local arrangements within the stochastic occupations of the lattice sites by chemically distinct atoms.

While the state of long-range order is determined by the sublattice compositions, the number of degrees of freedom of short-range order is in principle unbounded. In the simplest case of a binary system on a Bravais lattice, the Warren–Cowley short-range order parameters (Cowley 1950, Warren *et al* 1951) quantify the probabilities of pairs of sites being occupied by a given combination of elements. These pair-level correlations are accessible directly in the intensity variations of diffuse scattering, and both elastic neutron scattering (Schweika 1998) and x-ray scattering (Schönfeld 1999) in the diffuse regime have been used for determining short-range order in a range of systems.

Determination of long-range order via the intensities of Bragg and super-structure peaks is a routine experimental procedure (Inden and Pepperhoff 1990, Xiao and Baker 1995). In contrast, diffuse scattering experiments are much more labourious. This pertains even more for studies of short-range order in long-range ordered compounds, where after the pioneering work by Georgopoulos and Cohen (1981) on β'-NiAl not much information has been published. The richness of aspects of short-range order that can generally be expected in ordered compounds, including both correlations of the occupations of sites within a given sublattice and on distinct sublattices, might be a reason for this. Note that even in the above-mentioned example of β'-NiAl the occupational disorder is restricted to a single sublattice, which allowed it to be described within the conventional Bravais lattice formalism.

The outstanding properties of ordered intermetallics, including high yield strengths and high Young's moduli at low mass densities, corrosion resistance and high-temperature creep resistance (Sauthoff 1995, Pfeiler 2007), to name just a few, are due to the ordered arrangement of the atoms. However, lacking a detailed picture of local atomic arrangements, this has hitherto been considered only in terms of long-range order parameters. It is the aim of this work to take the first step towards a full model by generalizing the Warren–Cowley theory of short-range order to long-range ordered systems, thereby providing the necessary framework. Further, we will elucidate the accompanying phenomena by way of simulating temperature-dependent long- and short-range order. Specifically, we will consider the evolution of short-range order over an order-disorder transition in a non-stoichiometric B2 (CsCl) intermetallic alloy. We will assume a realistic potential in the vein of the embedded-atom method (EAM) (Daw and Baskes 1984). Such potentials are non-discrete, which allows us to compare simulations that explore the full classical parameter space including atomic displacements to simulations where the atoms are restricted to positions on an ideal lattice. To the best of our knowledge, this is the first time that short-range order resulting from a physically plausible, many-body phenomenological potential is derived.

The paper will be organized in the following way: in section 2, we will review the classical short-range order parameters and give a generalization for defining ordering on sublattices. We will detail the applied simulation technique in section 3, which will be followed by a discussion of the results in section 4 and a brief summary in section 5.

2. Theory

Warren and Cowley (Cowley 1950, Warren *et al* 1951, Cowley 1960) introduced parameters to quantify short-range order in binary systems. They can be defined as

$$\alpha_{lmn} = 1 - \frac{p_{lmn}^{\mathrm{AB}}}{c^{\mathrm{A}} c^{\mathrm{B}}}, \tag{1}$$

where c^{A} (c^{B}) is the overall concentration of atoms of type A (B) and p_{lmn}^{AB} is the probability that a given pair of sites separated by a lattice vector $\vec{r}_{lmn}$ is occupied by distinct atoms. These parameters were originally introduced to describe SRO in systems where no LRO is present. Without symmetry breaking, short-range interactions lead to correlations that decay with distance, so that for large separations the occupation of the sites is independent and therefore $p_{lmn}^{\mathrm{AB}} = c^{\mathrm{A}} c^{\mathrm{B}}$ and $\alpha_{lmn} = 0$.

Generally, the scattered intensity due to the sites of a Bravais lattice being occupied by different elements can be described by the expression (Schwartz and Cohen 2013)

$$I(\vec{q}) = \sum_{lmn} \alpha_{lmn} \cos(\vec{q} \cdot \vec{r}_{lmn}). \tag{2}$$

Here $\vec{q}$ denotes the position in reciprocal space, $\vec{r}_{lmn}$ are the lattice vectors, and the intensity is understood in terms of the Laue unit $c^{\mathrm{A}} c^{\mathrm{B}} (f^{\mathrm{A}} - f^{\mathrm{B}})^2$, where f^X is the $\vec{q}$-dependent scattering factor.

If the temperature compared to the ordering forces in the system is sufficiently low, a long-range superstructure lattice is formed. To give an example one may consider a B2 ordered system (ClCs structure), where the underlying body-centred cubic Bravais lattice dissociates into two simple cubic sublattices denoted as α and β. The long-range order parameter is given by the difference of the occupations of the sublattices

$$\eta = (c_\alpha^{\mathrm{A}} - c_\beta^{\mathrm{A}})^2 = (c_\alpha^{\mathrm{B}} - c_\beta^{\mathrm{B}})^2, \tag{3}$$

where c_χ^X is the concentration of element X on sublattice χ, that is, the probability that a given site on sublattice χ is occupied by an atom of element X.

With long-range order, the definition given in (1) will give non-zero values even for large $\vec{r}_{lmn}$. For a stoichiometric system with perfect order and no defects the short-range order parameter α_{lmn} is either -1 or 1, depending on whether $\vec{r}_{lmn}$ connects sites on the same or on different sublattices. In this case (2) gives δ-like superstructure peaks. The same is true for a long-range ordered system where the atomic concentration is non-stoichiometric, only that the excess atoms lead to the absolute value of the short-range order parameters being smaller than 1.

Specifically, assuming no short-range order we have

$$\begin{aligned} \bar{p}^{\mathrm{AB}} &= \frac{c_\alpha^{\mathrm{A}} c_\beta^{\mathrm{B}} + c_\alpha^{\mathrm{B}} c_\beta^{\mathrm{A}}}{2}, \\ \bar{p}^{\mathrm{AB}} &= \frac{c_\alpha^{\mathrm{A}} c_\alpha^{\mathrm{B}} + c_\beta^{\mathrm{A}} c_\beta^{\mathrm{B}}}{2} \end{aligned} \tag{4}$$

for atoms within different sublattices and for atoms within the same sublattice respectively. With the definition of η and (1) we get

$$\bar{\alpha}_{\xi\leftrightarrow\chi} = \pm\frac{\eta}{4c^{\mathrm{A}}c^{\mathrm{B}}}, \tag{5}$$

where the positive sign is for same sublattices ($\xi = \chi$) and the negative sign for different sublattices.

Under the presence of short-range order, the Warren–Cowley parameters for small $\vec{r}_{lmn}$ will reflect the actual short-range order, but for large separations they will converge to the appropriate limiting value of the above two. The short-range ordering can now be quantified by the difference of the actual value to the uncorrelated expression of (5)

$$\tilde{\alpha}_{lmn,\xi\leftrightarrow\chi} = \frac{c_\xi^{\mathrm{A}}c_\chi^{\mathrm{B}} - p_{lmn,\xi\chi}^{\mathrm{AB}}}{c^{\mathrm{A}}c^{\mathrm{B}}} = \frac{c_\xi^{\mathrm{B}}c_\chi^{\mathrm{A}} - p_{lmn,\xi\chi}^{\mathrm{BA}}}{c^{\mathrm{A}}c^{\mathrm{B}}}, \tag{6}$$

which indeed will converge towards zero after a small number of shells for non-critical temperatures. This allows the classical short-range order parameter to be written as a combination of a part that is due to long range order and a part that is strictly due to short-range ordering.

Note that for the B2 case considered here, with two inequivalent sublattices, for given *lmn* there are either two intra-sublattice short-range order coefficients or one inter-sublattice coefficient, corresponding to the cases:

$$\begin{aligned}\alpha_{lmn} &= \frac{\eta}{4c^{\mathrm{A}}c^{\mathrm{B}}} + \frac{\tilde{\alpha}_{lmn,\alpha\leftrightarrow\alpha} + \tilde{\alpha}_{lmn,\beta\leftrightarrow\beta}}{2},\\ \alpha_{lmn} &= -\frac{\eta}{4c^{\mathrm{A}}c^{\mathrm{B}}} + \tilde{\alpha}_{lmn,\alpha\leftrightarrow\beta}.\end{aligned} \tag{7}$$

3. Simulation

Configurations representative for the equilibrium configuration of the system were generated by the Metropolis–Hastings Monte Carlo method (Landau and Binder 2009). The internal energies of the specific configurations were computed according to the EAM-like potentials with long-range atomic interactions proposed by Ouyang *et al* (2012) for Fe–Al intermetallic alloys. For the two superstructures on the body-centred cubic lattice, the B2 phase with FeAl stoichiometry and the D0$_3$ phase with Fe$_3$Al stoichiometry, the resulting lattice constants, elastic constants, heat of fusion, point defect formation enthalpies, and the phonon dispersions were reported to agree very well with available experimental data (Ouyang *et al* 2012). In the following we will identify Fe with A and Al with B.

We implemented a grand-canonical Monte Carlo simulation, where a lattice site is chosen stochastically and its occupation is flipped with a probability that depends on the difference in the internal energies of the original and the flipped configuration and on a chemical potential. In order to achieve high efficiencies in the face of highly differing sublattice occupations, we allowed for a bias in attempt frequencies: specifically, if for a given sublattice the trial frequency for A → B swaps is $\omega_{\mathrm{A}\to\mathrm{B}}$ and analogously for the reverse transition, then performing the exchanges with probabilities

$$p_{X\to Y} = \min\left(1, \frac{\omega_{Y\to X}}{\omega_{X\to Y}}\exp\left(\frac{-\Delta H}{k_B T}\right)\right) \tag{8}$$

fulfills detailed balance (Hastings 1970). Note that here ΔH incorporates both the differences in internal energy as well as the effect of the chemical potential. We implemented this bias by keeping lists of the sites on each sublattice occupied by either element. Choosing $\omega_{\mathrm{A}\to\mathrm{B}}/\omega_{\mathrm{B}\to\mathrm{A}}$ approximately as $c_\xi^{\mathrm{B}}/c_\xi^{\mathrm{A}}$ (but fixed for the duration of the simulation) maximizes the acceptance rate and therefore the efficiency. We ensured the correct composition of the system via a temperature-dependent chemical potential. We simulate a physically meaningful evolution of time by incrementing at each trial with an exponentially-distributed random variable with a parameter according to the instantaneous trial frequency, which depends on the sublattice occupations.

We considered two statistical ensembles. The *on-lattice approach* constrains the atoms to their periodical lattice sites, so that the occupations of the sites are the only degrees of freedom. In the *off-lattice approach*, the atoms have the additional degree of freedom of deviating from their ideal positions. This was implemented by shifting random single atoms by random vectors and accepting the move with the Metropolis probabilities. As specific occupations of the lattice sites prefer specific off-lattice deviations (for instance, antistructure atoms of the larger element will lead to outward relaxations), allowing this degree of freedom slows down the occupational dynamics. We observed a slowing-down of about a factor of ten. Further, in the off-lattice simulations the lattice parameter was considered as an additional degree of freedom subject to Metropolis dynamics under zero external pressure, allowing the simulation cell to thermally fluctuate in size and to expand with increasing temperature.

We performed the averaging necessary to compute the simulated statistical parameters (such as the internal energy, lattice constant, sublattice occupations and pair distribution functions) by an exact temporal integral

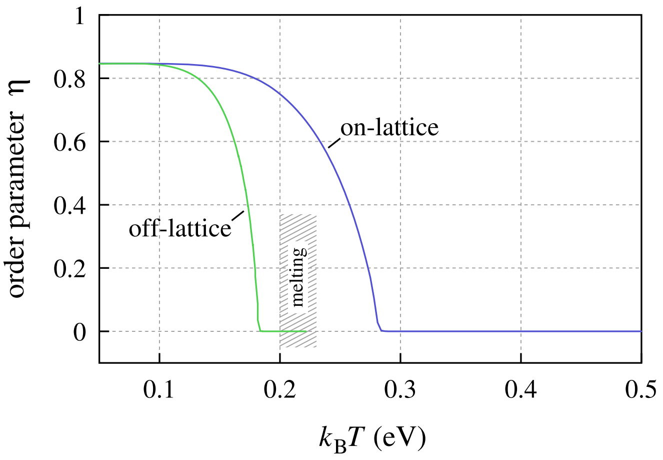

Figure 1. Long-range order parameter η as a function of temperature for on- and off-lattice approaches.

over the configurations as opposed to the conventional sampling approach. This was implemented by keeping records of the point in time a given quantity was changed the last time, and adding its value to the accumulating average with a weight given by the elapsed timespan when it is changed the next time. For the example of the pair distribution function, the neighbours of a flipped site are gone over, and the appropriate entry in the pair distributions is incremented proportional to the age of the pair, which is the minimum of the age of the two participating sites. Thanks to this approach and to the biasing discussed above, we can detect also correlations in defect species that become very small at low temperature, which would not be possible by a sampling approach.

The size of the system with periodic boundary conditions for the simulation cell was chosen to be $32^3 \times 2 = 65536$ atoms. By varying the simulation cell size, we have verified that this was large enough to avoid serious finite-size effects, which is also corroborated by the sharpness of the ordering phase transition we will report below. For being able to observe sizeable short-range order while still having access to large bcc and B2 phase regions, we used a composition of $c^\mathrm{A} = 54\%$ for the calculations. In the on-lattice case, we used a lattice constant of $a = 2.978$ Å at all temperatures, which is the low-temperature zero-pressure equilibrium value for this composition. No vacant sites were allowed.

Ideally, in the off-lattice case atoms are kept on their position in the lattice only by the interactions with their neighbours. At elevated temperatures this would give a non-zero possibility for the system to transition towards a neighbouring local minimum of the high-dimensional potential landscape even under the absence of point defects, corresponding to diffusional jumps via some mechanism of direct exchange. This would break neighbourhood relations and prohibit the computation of order parameters. Therefore, during atom displacements we enforced the constraint that the position of each atom in relation to its eight direct neighbours has to conform to the order relations on the lattice, specifically, along each dimension the coordinate of a given central atom has to be larger than those of the four neighbours on one side and smaller that those of the neighbour on the other side.

Of course, this constraint suppresses melting and leads to a different ensemble to be simulated. However, it is plausible that significant probabilities of such large displacements would lead to a melting of the unconstrained crystal, and indeed they appear only at temperatures where the lattice parameter has expanded by 3% and root-mean-square displacements with respect to the nearest neighbours have reached 18% of the nearest-neighbour distance. Following the Lindemann criterion (Grimvall and Sjödin 1974), we assume that the range of existence of the crystal has been covered and stop our simulation at this point. In contrast, in the on-lattice ensemble the atoms are fixed to their lattice sites so that crystals of arbitrarily large temperature can be considered and simulated.

4. Results

As the most obvious aspect of chemical ordering in the system, long-range order was calculated as a function of temperatures in keeping with (3). Results are shown in figure 1. They display the prototypical behaviour of Ising-like systems with only finite-energy excitations, so that the order parameter converges to its zero-temperature value faster than any power law. Specifically, below about 0.5 T_c the system is practically fully long-range ordered, that is, the α sublattice is occupied exclusively by A atoms, while the surplus of A atoms leads to constitutional antisites on the β sublattice.

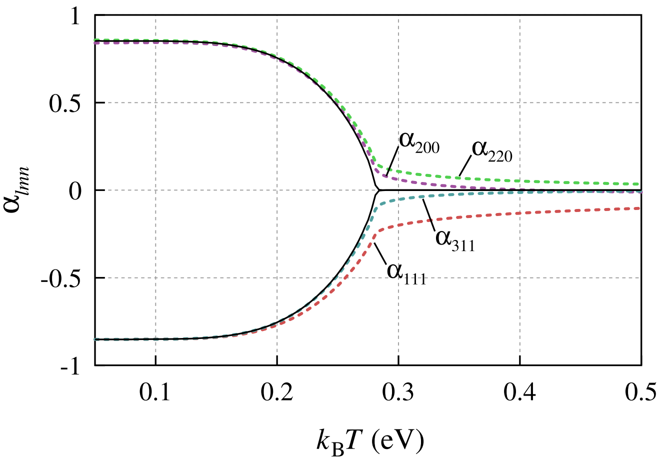

Figure 2. Classical short-range order parameter α_{lmn} as a function of temperature for the on-lattice approach. Values were calculated according to (1). The solid black lines correspond to the values under absence of local short-range ordering according to (5).

Further, it is evident that the choice of the statistical ensemble has a significant effect on the bcc ↔ B2 phase transition temperature, with $k_B T_c$ equal to 0.282 eV in the on-lattice case and about 0.183 eV in the off-lattice case. This is not surprising for two reasons: first, it is widely assumed (Fultz 2010) that oscillatory normal modes in a given system get softer with disorder, thereby increasing vibrational entropy and lowering the free energy of the disordered phase. Of course, the system has this freedom only in the off-lattice approach, which would imply a lowering of the critical temperature compared to the on-lattice case. Second, the relaxations around antistructure atoms mentioned above decrease their formation energy compared to the on-lattice case. This results in disorder being also less costly in energy in case of the off-lattice approach.

The temperature-dependent short-range order parameters for the first four neighbouring shells were calculated according to (1). The results are given in figure 2. It can be seen that at low temperatures, where the system is well ordered, the classical short-range order parameters do not deviate appreciably from the appropriate non-correlated values according to (5). This holds true even more for the inter-sublattice parameters, as the vanishing antisite concentration on the α sublattice c_α^B does not allow for any correlations to develop. For the intra-sublattice parameters very small deviations are discernible at low temperatures, which have to be due to short-range ordering of the constitutional antisites on the β sublattice. In contrast, on the high-temperature side sizeable short-range correlations are stable to the highest simulated temperatures, which, as was to be expected, are largest for closest neighbours.

While the classical short-range order parameters are sufficient to calculate the total occupational scattering according to (2), in the long-range ordered phase a large fraction of this intensity goes into the superstructure peaks. For discussing additional short-range order (or equivalently diffuse scattering), we also computed the sublattice-resolved short-range order coefficients according to (6). Results are shown in figure 3.

From the on-lattice results it is evident that above T_c the two sublattices are equivalent, and therefore the pertaining short-range order parameters are equal, and, as can be deduced from (7), they are also equal to the classical parameters in figure 2. Obviously also above T_c, the short-range order already hints at the eventual B2 symmetry breaking, as the inter-sublattice parameters are consistently negative, corresponding to a preference for pairs of unlike atoms if the sites are on different sublattices. Long-range order as illustrated in figure 1 obviously is not sensitive to these issues. *Mutatis mutandi*, the same holds for the intra-sublattice parameters. Here it is worth pointing out that, perhaps contrary to intuition, over a wide temperature range correlations over $\langle 220\rangle$ are stronger than those over $\langle 200\rangle$, even though the latter correspond to smaller separations.

The general behaviour of negative inter- and positive intra-sublattice short-range order parameters persists also some way below T_c, while the antisite concentration on the α-sublattice is becoming increasingly smaller and correlations between these antisites vanish. The constitutional antisites on the β-sublattice, on the other hand, develop a characteristic signature corresponding to an increasing preference for nearest-neighbour pairs of unlike atoms within the sublattice. This suggests that the system would undergo $D0_3$ ordering at even lower temperatures. Further, it is remarkable that up to a nonlinear rescaling of temperature, the off-lattice short-range order parameters behave quantitatively very similar to the on-lattice parameters.

The short-range order diffuse scattering intensity as given by (2) is depicted in figure 4. For the two chosen temperatures both above and below T_c, the diffuse scattering looks qualitatively very similar. However, while the intensity stays roughly constant at the Γ point, it decreases pronouncedly over the rest of the Brillouin zone during the ordering of the system. Note that the integrated scattering that is due to the sites of a lattice being

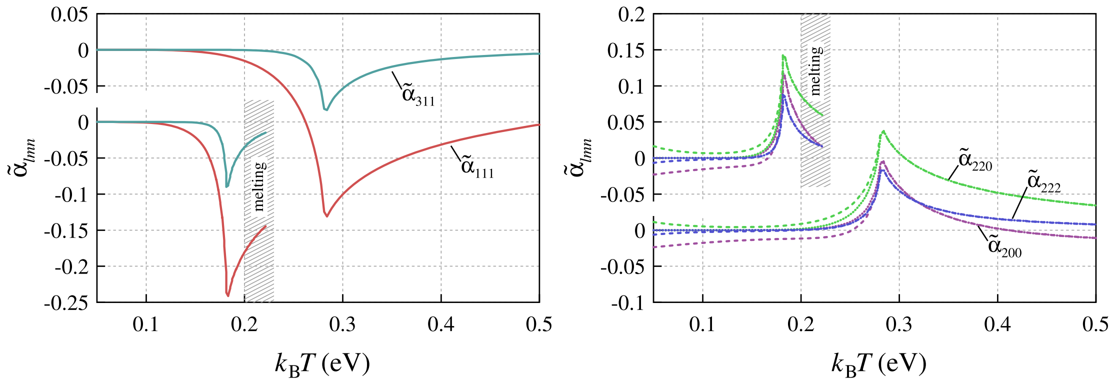

Figure 3. Sublattice-resolved chemical short-range order according to (6). Inter-sublattice ($\xi \neq \chi$) parameters are illustrated in the left panel, intra-sublattice ($\xi = \chi$) parameters in the right, where dashed lines represent parameters for the majority atom sublattice and dotted lines parameters for the minority atom sublattice with structural antisites at low temperatures. Off-lattice values are shifted with respect to on-lattice values, and drawn only up to the melting of the system.

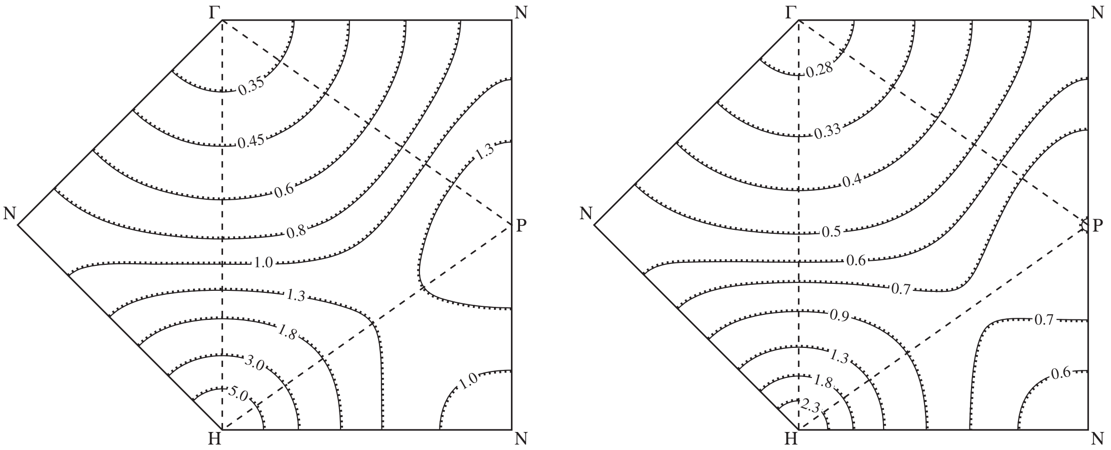

Figure 4. Diffuse scattering above (left) and below (right) the bcc ↔ B2 transition, computed in the on-lattice approach for $k_B T = 0.35$ eV and 0.25 eV, respectively. The intensity is depicted over all facets of the irreducible element of the bcc Brillouin zone (a model of which can be prepared by cutting and folding back along the dashed lines).

occupied by idealized point-like scatterers (as assumed in the definition of short-range order intensity) does not depend on the arrangement of the scatterers. When long-range ordering is present, the δ-like superstructure peaks compensate the reduction in short-range order diffuse scattering intensity. This is a consequence of a version of Parseval's theorem, which relates the squared l_2-norm of a function on a lattice (here the scattering lengths) to the squared L_2-norm of its Fourier transform (here the intensity). The Laue unit is chosen just so that the mean intensity is unity. If there is no long-range order, this directly holds also for the diffuse short-range order intensity. Under non-zero long-range order, on the other hand, the super-structure peaks account for a part of this scattered intensity, which in turn decreases the mean diffuse intensity.

Apart from the decrease in intensity, the figures also demonstrate that the short-range order diffuse scattering in general has only the periodicity of the reciprocal lattice of the Bravais lattice. In the present case, only at very low temperatures, where because of the vanishing antisite concentration on the α-sublattice all inter-sublattice parameters go to zero, the short-range order intensity would increasingly display the simple-cubic reciprocal-space symmetry of the B2 structure.

5. Conclusion

In the theoretical part of this work, we have shown how for long-range ordered systems the classical short-range order coefficients can be split into a term that depends only on the degree of long-range order and a term that is due to actual short-range order. The first term depends only on the sublattices the respective sites are on and does therefore not decay with distance. It is responsible for the sharp super-structure peaks. The second term represents deviations in the correlations in pair occupations from the long-range order term. For vectors in the structure's Bravais lattice, i.e. vectors that connect sites within a given sublattice, this short-range order term can further be written as a sum of parameters of correlations within the distinct sublattices.

Going beyond standard Metropolis simulations, we have presented an implementation of a Monte Carlo simulation in Hastings' framework, with a site-age based computation of the desired statistical quantities. These two complications allowed for an efficient study also of the very rare defects on the majority sublattice of an off-stoichiometric system. We simulated according to an EAM model of the Fe–Al system and demonstrated an increase in disordering temperature when constraining the atoms to the ideal lattice positions.

Finally, as an exemplary use of the formalism introduced in the first part of this work, we computed the evolution of the distinct short-range order coefficients with temperature, showing an increase of short-range order correlations with decreasing temperature in the disordered phase, with a maximum at the ordering temperature, and a successive decrease as the correlations become long-ranged. We also illustrated the corresponding diffuse scattering.

Additionally we could show that even though on-lattice and off-lattice simulation approaches show qualitatively similar results for ordering parameters, the differences can not be neglected.

Apart from exemplifying the concepts as done here, it is also conceivable to use simulations of diffuse scattering as substitutes for experimental data when short-range order information is necessary. Specifically, this pertains to the problem of data modelling in atomic-scale x-ray photon correlation spectroscopy (aXPCS) (Leitner 2012, Stana *et al* 2014), where in the simplest approximation (Leitner and Vogl 2011) the measured $\vec{q}$-dependent correlation times are a product of the short-range order diffuse scattering and a factor depending on the jump geometry. Only in rare cases (Leitner *et al* 2009) experimental short-range order data is available for the same composition and temperature range (Schönfeld *et al* 1999), or simple qualitative models such as nearest-neighbour site exclusions (Stana *et al* 2013) can describe the data. In the general case, simulations of the diffuse intensity as presented here can serve as a starting point for interpretation (Stana *et al* 2016). Further, studies as presented here can also be used to test potentials against each other or against experimental data, as the diffuse short-range order intensity is sensitive to minute details of the atomic interactions.

Acknowledgments

This research was funded by the Austrian Science Fund (FWF) contract P 28232. We also acknowledge the Scientific & Technological Cooperation project number PL 12/2015 and funding by the Deutsche Forschungsgemeinschaft (DFG) through TRR 80.

For support with the code our thanks go to Stephan Puchegger.

References

Cowley J 1960 *Phys. Rev.* **120** 1648–57
Cowley J M 1950 *Phys. Rev.* **77** 669–75
Daw M S and Baskes M I 1984 *Phys. Rev.* B **29** 6443–53
Fultz B 2010 *Prog. Mater. Sci.* **55** 247–352
Georgopoulos P and Cohen J 1981 *Acta Metall.* **29** 1535–51
Grimvall G and Sjödin S 1974 *Phys. Scr.* **10** 340
Hastings W K 1970 *Biometrika* **57** 97–109
Inden G and Pepperhoff W 1990 *Z. Met.* **81** 770–3
Landau D P and Binder K 2009 *A Guide to Monte Carlo Simulations in Statistical Physics* (Cambridge: Cambridge University Press) (doi:10.1017/CBO9780511994944)
Leitner M 2012 *Studying Atomic Dynamics with Coherent X-rays* (Berlin: Springer) (doi:10.1007/978-3-642-24121-5)
Leitner M, Sepiol B, Stadler L M, Pfau B and Vogl G 2009 *Nat. Mater.* **8** 717–20
Leitner M and Vogl G 2011 *J. Phys.: Condens. Matter* **23** 254206
Ouyang Y, Tong X, Li C, Chen H, Tao X, Hickel T and Du Y 2012 *Physica* B **407** 4530–6
Pfeiler W (ed) 2007 *Alloy Physics: A Comprehensive Reference* (New York: Wiley) (doi:10.1002/9783527614196)
Sauthoff G 1995 *Intermetallics* (New York: Wiley)
Schönfeld B 1999 *Prog. Mater. Sci.* **5** 435–543
Schönfeld B, Portmann M, Yu S and Kostorz G 1999 *Acta Mater.* **47** 1413–6
Schwartz L and Cohen J B 2013 *Diffraction from Materials* (Berlin: Springer) (doi:10.1007/978-3-642-82927-7)
Schweika W 1998 *Disordered Alloys: Diffuse Scattering and Monte Carlo Simulations* vol 141 (Berlin: Springer)
Stana M, Leitner M, Ross M and Sepiol B 2013 *J. Phys.: Condens. Matter* **25** 065401
Stana M, Ross M and Sepiol B 2014 Atomic migration studies with x-ray photon correlation spectroscopy *Recent Progress in Diffusion Thermodynamics and Kinetics in Intermetallic Compounds* ed R Kozubski vol 2 (Zürich: Trans Tech) pp 73–94
Stana M, Ross M and Sepiol B 2016 arXiv:1606.06516
Warren B E, Averbach B L and Roberts B W 1951 *J. Appl. Phys.* **22** 1493
Xiao H and Baker I 1995 *Acta Metall. Mater.* **43** 391–6